

# Low Utilization of Circulating Glucose after Food Withdrawal in Snell Dwarf Mice\*

Received for publication, January 17, 2007, and in revised form, September 4, 2007. Published, JBC Papers in Press, September 28, 2007, DOI 10.1074/jbc.M700484200

Natasha L. Brooks<sup>†1</sup>, Chad M. Trent<sup>†1</sup>, Carl F. Raetzsch<sup>‡</sup>, Kevin Flurkey<sup>§</sup>, Gunnar Boysen<sup>¶</sup>, Michael T. Perfetti<sup>‡</sup>, Yo-Chan Jeong<sup>¶</sup>, Simon Klebanov<sup>||</sup>, Kajal B. Patel<sup>‡</sup>, Valerie R. Khodush<sup>‡</sup>, Lawrence L. Kupper<sup>\*\*</sup>, David Carling<sup>††</sup>, James A. Swenberg<sup>¶</sup>, David E. Harrison<sup>§</sup>, and Terry P. Combs<sup>‡2</sup>

From the Departments of <sup>†</sup>Nutrition, <sup>¶</sup>Environmental Sciences and Engineering, and <sup>\*\*</sup>Biostatistics, University of North Carolina, Chapel Hill, North Carolina 27599, the <sup>§</sup>Jackson Laboratory, Bar Harbor, Maine 04609, <sup>||</sup>Columbia University College of Physicians & Surgeons, New York, New York 10025, and the <sup>††</sup>Medical Research Council Clinical Sciences Centre, Imperial College of London, London W12 0NN, United Kingdom

Glucose metabolism is altered in long-lived people and mice. Although it is clear that there is an association between altered glucose metabolism and longevity, it is not known whether this link is causal or not. Our current hypothesis is that decreased fasting glucose utilization may increase longevity by reducing oxygen radical production, a potential cause of aging. We observed that whole body fasting glucose utilization was lower in the Snell dwarf, a long-lived mutant mouse. Whole body fasting glucose utilization may be reduced by a decrease in the production of circulating glucose. Our isotope labeling analysis indicated both gluconeogenesis and glycogenolysis were suppressed in Snell dwarfs. Elevated circulating adiponectin may contribute to the reduction of glucose production in Snell dwarfs. Adiponectin lowered the appearance of glucose in the media over hepatoma cells by suppressing gluconeogenesis and glycogenolysis. The suppression of glucose production by adiponectin *in vitro* depended on AMP-activated protein kinase, a cell mediator of fatty acid oxidation. Elevated fatty acid oxidation was indicated in Snell dwarfs by increased utilization of circulating oleic acid, reduced intracellular triglyceride content, and increased phosphorylation of acetyl-CoA carboxylase. Finally, protein carbonyl content, a marker of oxygen radical damage, was decreased in Snell dwarfs. The correlation between high glucose utilization and elevated oxygen radical production was also observed *in vitro* by altering the concentrations of glucose and fatty acids in the media or pharmacologic inhibition of glucose and fatty acid oxidation with 4-hydroxycyanocinnamic acid and etomoxir, respectively.

Glucose metabolism is altered in centenarians and long-lived mice (1–8). Our current hypothesis is that a decrease in fasting glucose utilization may increase longevity by lowering oxygen

radical production, a potential cause of aging. Changes in glucose metabolism have been indicated in long-lived rodents by (a) oral glucose tolerance test, (b) insulin tolerance test, (c) inhibition of glucose production and stimulation of glucose disposal under euglycemic clamp conditions, and (d) the levels of circulating glucose and insulin under physiologic conditions (9–13). These methods suggest that glucose utilization is elevated in long-lived mice during feeding. However, they do not reveal whether glucose utilization is lower in long-lived mice during fasting, a period of the day when glucose utilization is relatively low and fatty acid utilization is high.

During fasting (a) the appearance in the circulation of glucose from the gastrointestinal tract is low, (b) the concentrations of circulating glucose and insulin are low, (c) circulating glucose is used for energy rather than storage, and (d) the circulating glucose used is replenished largely by liver glucose production, via gluconeogenesis and glycogenolysis. Thus, whole body glucose utilization may be lowered during fasting by decreasing glucose production. Whether fasting glucose production is decreased in long-lived mice is currently unknown.

Adiponectin, a hormone produced by adipose tissue, can lower glucose utilization by decreasing glucose production (14–16). Adiponectin is elevated in many long-lived mice (17, 18). The elevation of adiponectin in long-lived mice may also stimulate fatty acid utilization through its intracellular target, AMP-activated protein kinase (AMPK)<sup>3</sup> (19–21).

Reducing the utilization of glucose for energy may increase longevity by lowering the production of oxygen radicals from the mitochondria (22, 23). The link between glucose utilization and oxygen radical production is demonstrable in bovine aortic endothelial cells (24). Compared with 5 mM glucose, the incubation of aortic endothelia in 30 mM glucose doubled the rate of glucose utilization and tripled reactive oxygen species. The elevation of reactive oxygen species by 30 mM glucose was blocked by 4-hydroxycyanocinnamic acid (4-OHCA), an inhibitor of pyruvate transport into the mitochondria. The link between low glucose utilization and longevity is supported by the obser-

\* This work was supported by NIDDK, National Institutes of Health (NIH) Grants DK075573 and DK056350, NIA, NIH Grants AG025007 and AG18003, and NIEHS, NIH Grant ES10126. The costs of publication of this article were defrayed in part by the payment of page charges. This article must therefore be hereby marked "advertisement" in accordance with 18 U.S.C. Section 1734 solely to indicate this fact.

<sup>1</sup> Both authors contributed equally to this work.

<sup>2</sup> To whom correspondence should be addressed: Dept. of Nutrition, School of Medicine, School of Public Health, University of North Carolina, Chapel Hill, NC 27599-7461. Tel.: 919-966-7235; Fax: 919-966-7216; E-mail: terrycombs@unc.edu.

<sup>3</sup> The abbreviations used are: AMPK, AMP-activated protein kinase; 4-OHCA, 4-hydroxycyanocinnamic acid; ACC, acetyl-CoA carboxylase; ACM, adipocyte-conditioned media; FBS, fetal bovine serum; GC/MS, gas chromatography and mass spectrometry; HMT, hexamethylenetetramine; HS, horse serum; DMEM, Dulbecco's modified Eagle's medium; DN, dominant negative; EGFP, enhanced green fluorescent protein.

## Glucose Utilization and Longevity

vation that fasting glucose utilization in mice, rats, dogs, and humans, respectively, 20, 12, 4, and 2 mg/kg/min, correlates with the difference in longevity between these species (25–28).

In the present study, we set out to determine whether fasting glucose utilization is reduced in long-lived mice. We measured glucose utilization after food withdrawal in free moving long-lived Snell dwarf mice (29). We also investigated the mechanisms underlying the reduction of glucose utilization and whether low glucose and high fatty acid utilization could reduce oxygen radical production.

### EXPERIMENTAL PROCEDURES

**Mouse Models**—All mice were 4- to 7-month-old males. Snell dwarf and control mice were food-deprived after 7 a.m. and all measurements were made at 1–3 p.m. Snell dwarf and control mice were F1 hybrids from female DW/J (Pit1<sup>dw/+</sup>), and male C57Bl/6J (Pit1<sup>dw/+</sup>) Snell dwarfs were housed with controls. Adiponectin transgenic mice were previously described (16). Autoclaved NIH3 chow (Diet 96WA: 73% carbohydrate, 18% protein, 4% fat, 5% ash) and acidified water were provided. Temperature (23 °C), humidity (55%), and a 12-h light/12-h dark cycles were strictly controlled. Procedures were approved by the Institutional Animal Care and Use Committees of the Jackson Laboratories and the University of North Carolina.

**Glucose Utilization in Vivo**—Due to the small size of Snell dwarf mice, glucose utilization was measured by single injection of tracer instead of the primed infusion technique (30). Trace amounts of carbon-3-labeled [<sup>3</sup>H]glucose (PerkinElmer Life Sciences) in saline (50–100  $\mu$ l) were injected directly into the circulation of conscious free moving mice through the ophthalmic plexus (31). Blood samples (10–20  $\mu$ l) were collected from the tail tip at 3, 6, 9, 12, 15, 18, and 21 min after injection for the measurement of (a) glucose by a hand-held glucose meter and (b) radioactivity by scintillation counter (15, 16). The glucose meter (Johnson & Johnson) showed comparable accuracy and reproducibility to colorimetric assays. High-performance liquid chromatography analysis was performed to verify that the radioactivity measured in dried plasma by scintillation counter represented [<sup>3</sup>H]glucose. We used an Agilent 1100 high-performance liquid chromatography system connected to a beta-RAM Model 2B Detector (IN/US Systems) and an Aminex HPX-87C polystyrene divinylbenzene resin column (Bio-Rad) at 80 °C using a 0.6 ml/min flow of water. Blood collected immediately before [<sup>3</sup>H]glucose injection was used to measure insulin and adiponectin by radioimmunoassay (Linco) and Western blot analysis, respectively (17). Mutant and control mice were always paired for the measurement of glucose utilization.

**Calculations**—The disappearance of radioactivity in plasma exhibited single phase exponential kinetics according to  $\ln(E_i) = -kt + \ln(E_0)$ , where  $E_i$  is [<sup>3</sup>H]glucose in plasma at time  $i$ ,  $k$  is the fractional elimination constant ( $\text{min}^{-1}$ ),  $t$  is the time after [<sup>3</sup>H]glucose injection (min), and  $E_0$  is the initial [<sup>3</sup>H]glucose in plasma at time 0. Glucose utilization was calculated by multiplying  $k$  with the total pool of circulating glucose ( $Q$ ) and dividing by the body weight (32). The pool of circulating glucose was estimated from the initial dilution of the tracer.

**Contribution of Gluconeogenesis and Glycogenolysis to Glucose Production**—Plasma glucose produced by gluconeogenesis and glycogenolysis was measured in free moving Snell dwarf and control mice by measuring <sup>2</sup>H enrichment of plasma glucose on carbons 5 and 2 (33). Enrichment (~5%) of body water by <sup>2</sup>H<sub>2</sub>O was achieved by intraperitoneal injection of <sup>2</sup>H<sub>2</sub>O (0.015  $\times$  body weight) and the provision of 5% <sup>2</sup>H<sub>2</sub>O drinking water at 10 a.m. The <sup>2</sup>H<sub>2</sub>O enrichment of body water was confirmed by mixing plasma, collected 1–3 p.m., with calcium carbide to form acetylene gas (34). Acetylene gas was analyzed by GC/MS using an EC5 Alltech Econo-CAP column (30 m  $\times$  0.32 mm, film thickness of 1  $\mu$ m) at 200 °C. Acetylene and [<sup>2</sup>H]acetylene were measured by monitoring  $m/z$  26 and 27, respectively. To measure <sup>2</sup>H enrichment of circulating glucose on carbons 5 and 2, plasma (100  $\mu$ l) was deproteinated by ZnSO<sub>4</sub>/Ba(OH)<sub>2</sub> and deionized through an AG-1-X8 (COO<sup>-</sup> form) over an AG-50W-X8 (H<sup>+</sup> form) resin column (Bio-Rad). For the measurement of <sup>2</sup>H labeling of glucose on carbon 5, glucose (50  $\mu$ g) was converted to xylose. Oxidation yielded formaldehyde that contained carbon 5 of glucose and its hydrogen. Six formaldehydes in NH<sub>4</sub>OH were condensed to produce solid hexamethylenetetramine (HMT). HMT was dissolved in dichloromethane and analyzed by GC/MS using an EC5 Alltech Econo-CAP column (30 m  $\times$  0.32 mm, film thickness of 1  $\mu$ m) operated at 60 °C for 1 min followed by an increase to 300 °C at 10 °C/min under 2 ml/min He<sub>2</sub> gas. HMT and [<sup>2</sup>H]HMT were measured by single ion monitoring of  $m/z$  140 and 141, respectively. For the measurement of <sup>2</sup>H labeling of glucose on carbon 2, glucose (10–20  $\mu$ g) was reduced to sorbitol with NaHB<sub>4</sub>. The hydrogen on carbon 2 was transferred to lactate using sorbitol dehydrogenase and lactate dehydrogenase (Sigma). Lactate was derivatized and analyzed by GC/MS using a Pal A200 autosampler (Leap) and a Trace GC-2000 attached to a TSQ 7000 mass analyzer (ThermoFinnigan) under He<sub>2</sub> gas (2 ml/min). *In vivo* measurements of gluconeogenesis were estimated by using carbon 5/carbon 2 enrichment instead of carbon 5/body water <sup>2</sup>H<sub>2</sub>O to eliminate the diluting effect of glucose absorption from the gastrointestinal tract.

**Glucose in Stomach Contents**—Stomach contents were isolated from Snell dwarf and control mice after euthanasia and analyzed for glucose (35). In brief, stomach contents (50–250 mg) were digested in 1 N NaOH, and protein was precipitated out with 1 N perchloric acid. Glycogen was precipitated out of solution in ethanol and digested with 1 mg/ml amyloglucosidase (Sigma) in 0.5 M sodium acetate (pH 4.5) for 4 h at 55 °C before glucose was measured by colorimetric assay (Waco).

**Body Composition**—Percent body fat and body water were measured in conscious mice by magnetic resonance imaging using an Echo magnetic resonance imaging-100 QNMR system. Percentages of body fat and body water were also estimated from the radioactivity in a sample of plasma 1 h after <sup>3</sup>H<sub>2</sub>O injection for verification.

**Glucose Production in Vitro**—Glucose production in McArdle 7777 rat hepatoma cells was determined as previously described with minor modifications (14). Cells were thawed from liquid nitrogen storage upon rat tail collagen I-coated plates. Cells equilibrated for 24 h in high glucose (25 mM) Dulbecco's Modified Eagle Medium (DMEM) supplemented with

2.5% fetal bovine serum (FBS) and 2.5% horse serum (HS). After equilibration, cells were split into 12-well plates at a density of  $2.5 \times 10^4$  cells/well and allowed 2–3 h for adherence. The media was changed to serum-free low glucose (5 mM) DMEM. After 8 h, adipocyte conditioned media (ACM) with or without adiponectin (ACM-adiponectin) was added. Media and cell lysates were collected 8 h later. Colorimetric assay kits were used to determine glucose in the media (Waco) and cell protein content (Pierce). ACM-adiponectin was produced by depleting adiponectin from ACM by immunoprecipitation using rabbit antisera produced with the peptide antigen EDDVTTEELAPALV, representing adiponectin residues 18–32. Preimmune rabbit serum was used as a control.

**Retroviral Transduction in Vitro**—A DNA construct encoding a dominant negative AMPK mutant (DN-AMPK) was used to generate a 5'-EcoRI/3'-SacII DN-AMPK fragment (36). The fragment was cloned into a retroviral shuttle vector pML<sub>2</sub>(EGFP-N1) producing DN-AMPK-pML<sub>2</sub>(EGFP-N1). HEK293 cells were transfected with a 3:1 ratio of DN-AMPK-pML<sub>2</sub>(EGFP-N1) and pCL-Eco, encoding the ecotropic envelope protein (Imgenex), using FuGENE transfection reagent (Roche Applied Science). HEK293 cells were incubated at 37 °C for 48 h. Media was changed, and cells were placed at 32 °C for 48 h to allow for retroviral production. The media containing virus (6 ml) was mixed with Polybrene (2.67 μg) and centrifuged at 3500 rpm for 5 min at room temperature. The supernatant was introduced to actively growing hepatoma cells (2 ml/well of 6-well plate) for 12–18 h at 37 °C. Medium was replaced with DMEM/FBS/HS. Overexpression of DN-AMPK was verified by EGFP and PCR (data not shown). The pML<sub>2</sub>(EGFP-N1) construct was used as a control for effects of retroviral transduction.

**Fatty Acid Utilization in Vivo**—Trace amounts of carbon-1-labeled [<sup>14</sup>C]oleic acid (PerkinElmer Life Sciences) were dried under nitrogen gas and allowed to equilibrate in plasma for 1 h at 37 °C. The utilization of circulating oleic acid was measured in conscious free moving Snell dwarf and control mice by injecting [<sup>14</sup>C]oleic acid directly into the circulation through the ophthalmic plexus. Blood samples (25–50 μl) were collected from the tail tip at 5, 15, 30, 55, and 70 min after injection to measure (a) free fatty acids by colorimetric assay (Waco) and (b) radioactivity by scintillation counting (16). To verify that the radioactivity in plasma represented [<sup>14</sup>C]oleic acid, high-performance liquid chromatography analysis was performed at room temperature on a Zorbax SB-Aq column (Agilent) under 1.5 ml/min 90:9:1 acetonitrile:water:acetic acid. GC/MS analysis revealed oleic acid represented ~15–16% of circulating fatty acids in Snell dwarf and control mice in the 0- and 70-min blood samples (37). Snell dwarf and control mice were always paired for the measurement of fatty acid utilization. The measurement of glucose and fatty acid utilization by [<sup>3</sup>H]glucose and [<sup>14</sup>C]oleic injection was based on similar tracer analysis assumptions, including: 1) the tracer is homogeneously mixed in the circulation, 2) the tracer is metabolically indistinguishable from glucose or oleic acid, and 3) the production of [<sup>14</sup>C]oleic acid or [<sup>3</sup>H]glucose by isotope exchange is insignificant.

**Intracellular Triacylglycerol and Acetyl-CoA Carboxylase**—Intracellular triacylglycerol content in liver and heart was determined by homogenizing freeze-clamped tissue stored at –80 °C in 2:1 chloroform/methanol. Briefly, tissue homogenates were mixed with 0.9% NaCl before the lipid extract was dried and analyzed for triacylglycerol by enzymatic colorimetric assay (Waco). Liver acetyl-CoA carboxylase (ACC) and phosphorylated ACC was measured by Western blot analysis (17). Antibodies against ACC were commercially available (Cell Signaling).

**Protein Carbonyl Content**—Protein carbonyl groups were derivatized with 2,4-dinitrophenylhydrazine, producing dinitrophenylhydrazone products that were quantified by spectrophotometric analysis (38). Mouse liver and McArdle 7777 rat hepatoma cells were analyzed according to the manufacturer's protocol for the Protein Carbonyl Assay Kit (Cayman Chemical). Mouse liver (50–150 mg) was homogenized in 2.5 M hydrochloric acid with or without 2,4-dinitrophenylhydrazine. Rat hepatoma cells were scraped off collagen-coated plates, split in two tubes, and centrifuged at 14,000 rpm for 5 min at 4 °C. Cell pellets were either dissolved in 2,4-dinitrophenylhydrazine or 2.5 M HCl. Samples were vortexed and incubated in the dark for 1 h at room temperature. Homogenates received 20% trichloroacetic acid and incubated on ice for 5 min. Samples were centrifuged at 14,000 rpm for 10 min at 4 °C. Pellets were dissolved in 10% trichloroacetic acid and incubated 5 min on ice. Samples were centrifuged at 14,000 rpm for 10 min at 4 °C. Pellets were dissolved in ethanol:ethyl acetate (1:1). Samples were centrifuged at 14,000 rpm for 10 min at 4 °C. Pellets were resuspended in guanidine-HCl and centrifuged at 14,000 rpm for 10 min at 4 °C. The supernatant was split and analyzed by a spectrophotometer (415 nm). Protein concentrations were determined by BCA assay (Pierce).

**Glucose versus Fatty Acid Utilization in Vitro**—Rat hepatoma cells were thawed from frozen vials into DMEM/FBS/HS. Cells were allowed to adhere overnight onto plastic tissue culture plates and split into 12-well plates ( $2.5 \times 10^4$  cells/well). Medium was removed after 24 h, and cells were treated with high glucose media (20 or 40 mM). The final media contained 0 or 0.5 mM oleic acid, 1% fat-free bovine serum albumin, 0.1 mM L-carnitine, and 0, 0.1 or 1.0 mM etomoxir (Sigma). Glucose and oleic acid in the media offered cells two sources of calories.

**Steady-State Levels of H<sub>2</sub>O<sub>2</sub> per ATP in Bovine Aortic Endothelial Cells**—Bovine aortic endothelial cells were plated at  $5 \times 10^4$  cells/well in DMEM/30 mM glucose and HS/FBS for 16 h followed by DMEM/5 mM glucose for 8 h. Cell medium was replaced with DMEM/5 mM glucose/1 mM carnitine/0.1 mM oleate/[<sup>14</sup>C]oleate/1% bovine serum albumin (fatty acid free). 4-Hydroxycyanocinnamic acid (Bruker) was included in the final media at concentrations indicated. Cells were harvested after 8 h to measure steady-state levels of H<sub>2</sub>O<sub>2</sub> by colorimetric assay (BioAssay Systems) and ATP by luminescence assay (Promega). The media was mixed with perchloric acid (5:1) to isolate [<sup>14</sup>C]-labeled acid-soluble metabolites (ketone bodies) and estimate β-oxidation (39).

**Statistical Analysis**—Student's *t* test was used to identify significant differences when data within groups showed a normal

## Glucose Utilization and Longevity

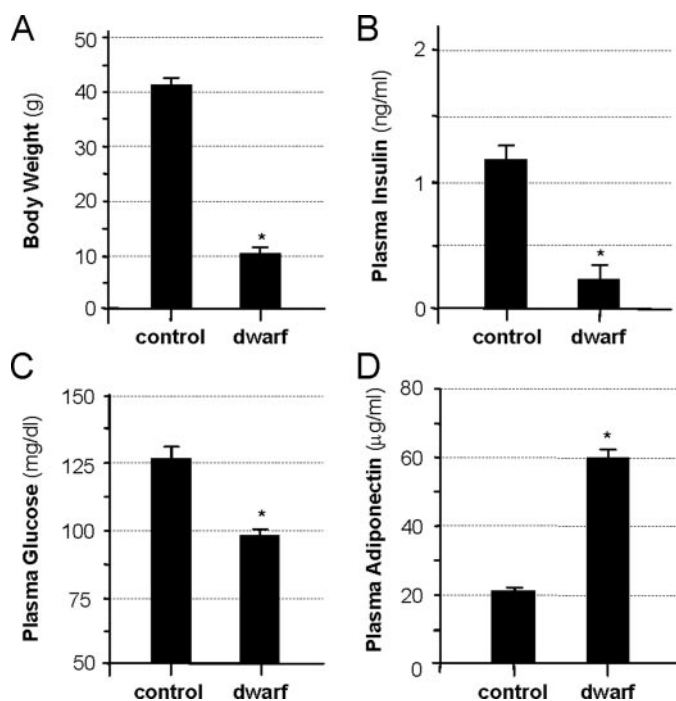


FIGURE 1. Physiologic features of long-lived Snell dwarf mice. *A*, body weight; *B*, insulin; *C*, glucose; and *D*, adiponectin for control and Snell dwarf mice. Mice were denied access to food at 7 a.m. Measurements were made at 1–3 p.m. Bars represent mean  $\pm$  S.E. ( $n = 6$ ). \*, significant difference between Snell dwarf and control mice ( $p < 0.05$ ).

distribution and Wilcoxon-Rank Sum test was used when data did not show a normal distribution.  $p$  values less than 0.05 were considered significant.

## RESULTS

Reduced body weight, insulin, glucose, and elevated adiponectin were observed in Snell dwarf mice (Fig. 1). The elevation of insulin sensitivity in Snell dwarfs is evident on the basis of the homeostatic model assessment representing the product of fasting glucose and insulin values divided by a species-specific constant.

The utilization rate of plasma glucose was 60% lower in Snell dwarf mice than their litter mate controls ( $3.6 \pm 0.4$  versus  $9.2 \pm 1.0$  mg/kg/min,  $p < 0.05$ , Fig. 2*A*). During the measurement of glucose utilization, the stomach of Snell dwarf and control mice contained small amounts of amylase digestible starch (Fig. 2*B*). Therefore, in addition to gluconeogenesis and glycogenolysis, the absorption of glucose from the gastrointestinal tract may have contributed to the production of plasma glucose. Snell dwarf and control mice were 21–25% body fat by magnetic resonance imaging. The level of radioactivity measured in plasma after  $^3\text{H}_2\text{O}$  injection supported that percent body fat was similar between Snell dwarf and control mice. We further investigated (*a*) the mechanisms that suppressed glucose utilization and (*b*) the possible link between low glucose utilization and longevity.

Low utilization of plasma glucose indicates a low rate of glucose production is needed to maintain a stable concentration of circulating glucose. Thus, we inquired whether the production of plasma glucose was suppressed by the inhibition of glucono-

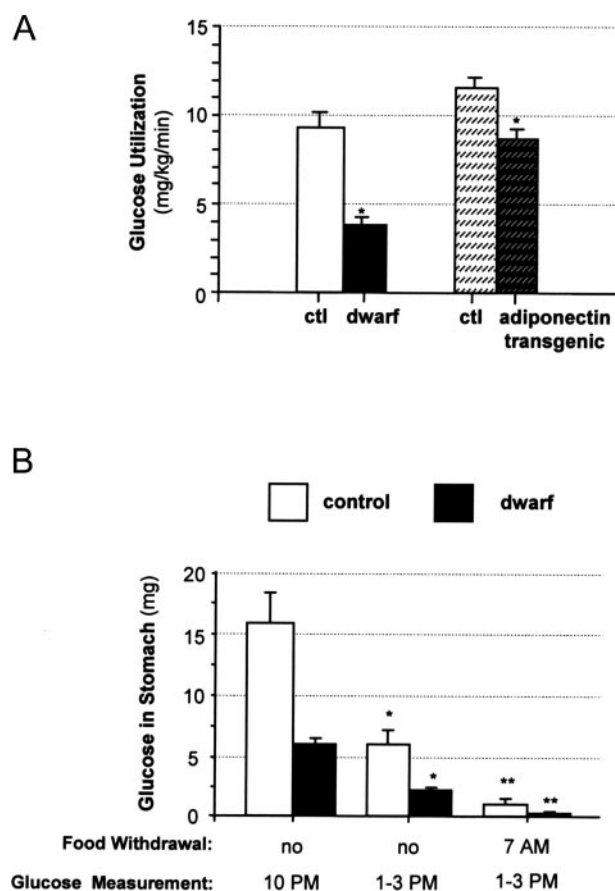
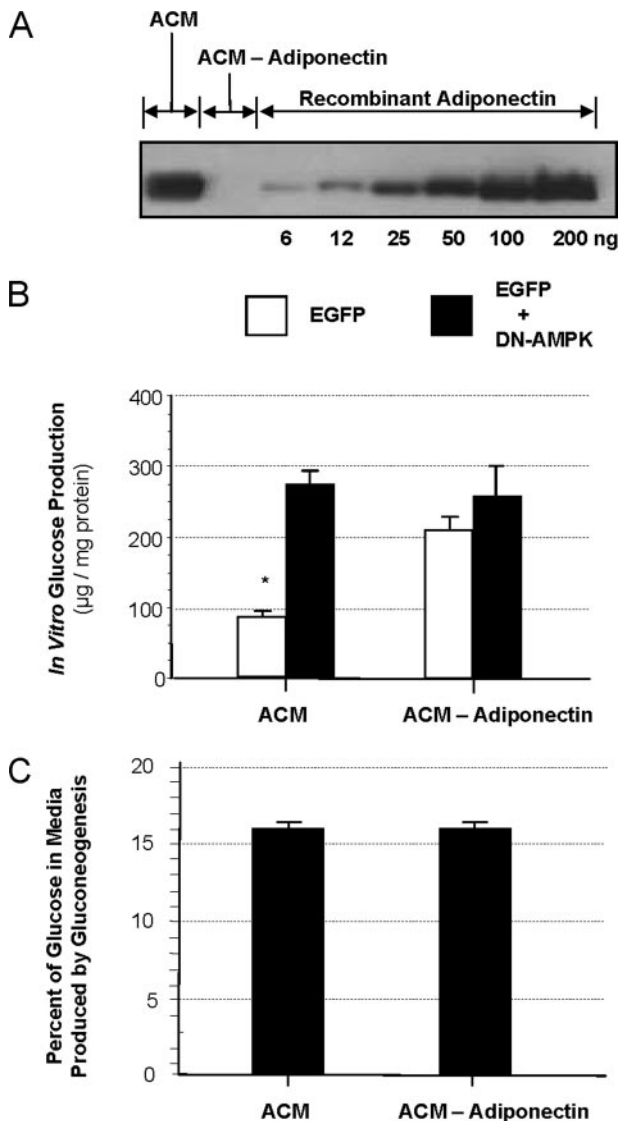


FIGURE 2. Low fasting glucose utilization in Snell dwarf and adiponectin transgenic mice. *A*, fasting glucose utilization was determined by [ $^3\text{H}$ ]glucose injection. Bars represent mean  $\pm$  S.E. ( $n = 6$ ). \*, significant difference between mutant and control (*ctl*) mice ( $p < 0.05$ ). *B*, glucose in the stomach contents of control and Snell dwarf mice. Bars represent mean  $\pm$  S.E. ( $n = 4$ ). \* and \*\*, significantly different from group shown immediately to the left ( $p < 0.05$ ).

genesis and glycogenolysis, the main sources of glucose in the fasting state.  $^2\text{H}$  labeling of plasma glucose by  $^2\text{H}_2\text{O}$  indicated that 50% of endogenous glucose production was derived by gluconeogenesis and 50% by glycogenolysis in both Snell dwarf and control mice. Therefore, glucose production in Snell dwarf mice was suppressed by a mechanism that did not change the percentage of glucose from gluconeogenesis and glycogenolysis.

Low fasting glucose utilization in Snell dwarfs was considered to be an effect of elevated adiponectin as seen in adiponectin transgenic mice (Fig. 2*A*). The possibility that adiponectin contributed to the suppression of glucose utilization was tested further in hepatoma cells exposed to 3T3-L1 ACM either with or without adiponectin (ACM-adiponectin). Adiponectin did not suppress glucose production in cells expressing a dominant negative form of AMPK (Fig. 3*B*). Isotope labeling of glucose by  $^2\text{H}_2\text{O}$  indicated that 16% of glucose in the media was produced by gluconeogenesis regardless of whether cells were exposed to ACM or ACM-adiponectin (Fig. 3*C*). Thus, adiponectin suppressed glucose production *in vitro* without changing the percent glucose produced from gluconeogenesis and glycogenolysis.



**FIGURE 3. Adiponectin inhibits glucose production by AMPK but does not change the percent glucose produced by gluconeogenesis.** *A*, Western blot analysis showing adiponectin in 3T3-L1 adipocyte-conditioned media (ACM). The first lane (left) shows adiponectin immunoprecipitated from 1 ml of ACM. The second lane shows the absence of adiponectin after immunoprecipitation from ACM (ACM-adiponectin). The remaining lanes show 6, 12, 25, 50, 100, and 200 ng of recombinant murine adiponectin. *B*, adiponectin cannot suppress glucose production *in vitro* without AMPK. Hepatoma cells were transfected with retrovirus encoding either EGFP (white) or EGFP and dominant negative AMPK (DN-AMPK, black). Bars represent mean  $\pm$  S.E. ( $n = 3$ ). \*, significant difference between ACM and ACM-adiponectin ( $p < 0.05$ ). *C*, percent glucose produced by gluconeogenesis does not differ between ACM and ACM-adiponectin exposure. Bars represent mean  $\pm$  S.E. ( $n = 3$ ).

The utilization rate of oleic acid, a long-chain fatty acid, was higher in Snell dwarf mice than control mice (Fig. 4A). Oleic acid utilization was determined by measuring the disappearance of radioactivity in plasma after trace amounts of [ $^{14}\text{C}$ ]oleic acid were injected into the circulation. GC/MS analysis revealed that oleic acid represented 15–16% of circulating fatty acids in both Snell dwarf and control mice. Other indications that fatty acid oxidation was elevated in Snell dwarfs included the reduction of intracellular triacylglyceride contents in liver and heart (Fig. 4B) and elevated ACC phosphorylation in the liver (Fig. 4C).

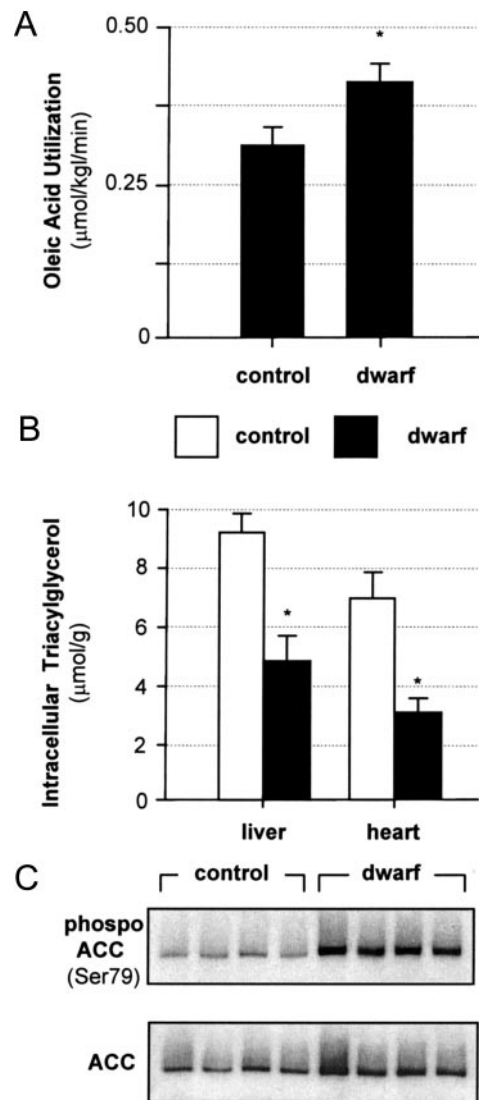


**FIGURE 4. High fatty acid utilization in fasting Snell dwarf mice.** *A*, fasting long-chain fatty acid utilization determined by [ $^{14}\text{C}$ ]oleic acid injection. Bars represent mean  $\pm$  S.E. ( $n = 5$ ). \*, significant difference between controls and Snell dwarfs ( $p < 0.05$ ). *B*, low intracellular triacylglyceride content in Snell dwarf liver and heart. Each bar represents mean  $\pm$  S.E. ( $n = 5$ ). \*, significant difference between controls and Snell dwarfs ( $p < 0.05$ ). *C*, elevated ACC phosphorylation in Snell dwarf livers by Western blot analysis. Significant increases in ACC phosphorylation (normalized to total ACC) were observed in Snell dwarfs by densitometry ( $p < 0.05$ ).

In comparison to control mice, Snell dwarfs showed a reduction in the protein carbonyl content of the liver (Fig. 5A). The protein carbonyl content in hepatoma cells was increased by elevated glucose and the absence of fatty acids in the media. The protein carbonyl content in hepatoma cells was also elevated by etomoxir, an inhibitor of fatty acid oxidation (Fig. 5B).

Our observations in Snell dwarfs and hepatoma cells suggested that the switch from glucose to fatty acid utilization after food withdrawal may reduce oxygen radical production. We are unaware of any previous studies that tested whether the aerobic metabolism of glucose can lead to greater oxygen radical production than the aerobic metabolism of fatty acids. Thus, we also measured steady-state levels of  $\text{H}_2\text{O}_2$  per ATP in primary bovine aortic endothelial cells. 4-OHCA, a pyruvate transport

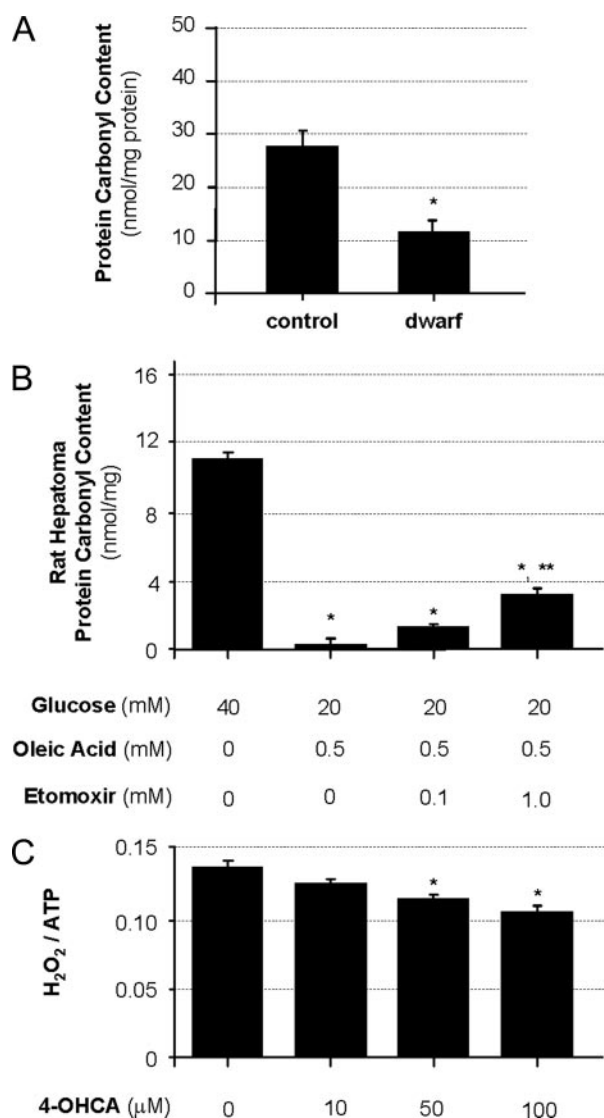


**FIGURE 5. Protein carbonyl content, a marker of oxygen radical damage, is decreased in Snell dwarf mice and elevated *in vitro* by high glucose utilization.** *A*, liver protein carbonyl content in Snell dwarf and control mice. Bars represent mean  $\pm$  S.E. ( $n = 6-7$ ). \*, significant difference between Snell dwarfs and controls ( $p < 0.05$ ). *B*, protein carbonyl content in rat hepatoma cells exposed to the indicated concentrations of glucose, oleic acid, and etomoxir, an inhibitor of fatty acid oxidation. Bars represent mean  $\pm$  S.E. ( $n = 3$ ). \*, significantly different from high glucose/fatty acid free media ( $p < 0.05$ ); \*\*, significantly different than lower concentrations of etomoxir ( $p < 0.05$ ). *C*, steady-state levels of H<sub>2</sub>O<sub>2</sub> per ATP in primary bovine aortic endothelial cells. 4-OHCA, a pyruvate transport inhibitor used to block the aerobic metabolism of glucose, lowered H<sub>2</sub>O<sub>2</sub> production per ATP. Bars represent mean  $\pm$  S.E. ( $n = 3$ ). \*, significantly different from control ( $p < 0.05$ ); \*\*, significantly different from lower concentration of 4-OHCA ( $p < 0.05$ ).

inhibitor, lowered H<sub>2</sub>O<sub>2</sub> per ATP (Fig. 5C). 4-OHCA increased fatty acid oxidation, estimated by ketone body production (data not shown).

The reduction of circulating glucose in Snell dwarf mice also led us to examine whether the frequency of glycations, nonenzymatic glycosylation reactions associated with diabetic complications and aging, was decreased. However, hemoglobin A1c, produced by the glycation of N-terminal valines on the  $\beta$ -chain of hemoglobin, was similar in Snell dwarf and control mice (4–5%).

## DISCUSSION

Our tracer analysis indicates that fasting glucose utilization is reduced in long-lived Snell dwarf mice. Fasting glucose utilization may be reduced by several mechanisms. Low insulin in Snell dwarfs can decrease insulin-mediated utilization of glucose by insulin-responsive tissues, mainly muscle and adipose (40, 41). Growth hormone, insulin-like growth factor-1, and thyroid hormone deficiency in Snell dwarfs can lower tissue demand for glucose (42, 43). A decrease in the production of plasma glucose may also lower fasting glucose utilization (26, 44).

The elevation of adiponectin in Snell dwarf mice may increase insulin inhibition of glucose production and thereby contribute to the reduction of fasting glucose utilization. Euglycemic clamp experiments previously showed that rapid elevation of adiponectin, 3-fold over baseline, increases insulin inhibition of glucose production without altering insulin-mediated glucose uptake (15). Euglycemic clamp experiments showed the same result in adiponectin transgenic mice that exhibit a chronic 3-fold elevation of adiponectin (16). The reduction of fasting glucose utilization observed in adiponectin transgenic mice, in the present study, suggests that the 3-fold elevation of adiponectin in Snell dwarfs is exerting an inhibitory effect on glucose production during fasting (Fig. 2A). *In vitro* data, presented here and elsewhere, obtained under conditions that resemble the fasting state (low glucose and insulin), support the hypothesis that adiponectin lowers glucose production during fasting (14).

Glucose production can be suppressed by the reduction of gluconeogenesis or glycogenolysis (45, 46). Our *in vivo* isotope labeling analysis indicated that the suppression of glucose production in Snell dwarfs is mediated without any change in the percent glucose from gluconeogenesis and glycogenolysis. Our *in vitro* isotope-labeling studies also indicated that adiponectin lowers glucose production without altering the percent glucose from gluconeogenesis and glycogenolysis. Thiazolidinediones, pharmacologic agents widely prescribed for the treatment of insulin resistance in type-2 diabetics, increase adiponectin and lower fasting glucose utilization (47, 48). These observations support that elevated adiponectin may contribute to the reduction of glucose production in Snell dwarfs and possibly other long-lived models that exhibit elevated adiponectin (17, 18).

Previous studies in mice show that adiponectin suppression of glucose production can be blocked by the ablation of the AMPK gene (49). We showed that the inhibition of glucose production by adiponectin *in vitro* was blocked by the expression of a dominant negative AMPK mutant (36). Studies in isolated hepatocytes showed the inhibition of AMPK can block adiponectin suppression of mRNA encoding phosphoenolpyruvate carboxykinase and glucose-6-phosphatase, two rate-limiting enzymes in gluconeogenesis (20).

AMPK activation by adiponectin may also play a role in the elevation of fatty acid utilization in Snell dwarf mice. AMPK phosphorylates ACC and malonyl-CoA decarboxylase, lowering malonyl-CoA, a precursor in fatty acid synthesis and potent inhibitor of mitochondrial carnitine palmitoyltrans-

ferase-1, the long-chain fatty acyl-CoA transporter (50). In the present study, increased phosphorylation of ACC is consistent with the elevation of fatty acid utilization and the reduction of intracellular lipid stores in Snell dwarf liver and heart (Fig. 4). Gene expression array data in Snell dwarf and other long-lived mice, including the Ames dwarf, little, and growth hormone receptor-null mice, support the conclusion that fatty acid oxidation is elevated in these long-lived mice (51).

Whether the aerobic metabolism of glucose leads to more oxygen radical production than fatty acid oxidation is not known. We present three results that suggest glucose and fatty acid oxidation could differentially affect oxygen radical production: 1) low glucose and high fatty acid utilization correlated with a low level of oxygen radical damage in Snell dwarf mice (Fig. 5A), 2) oxygen radical damage increased with the elevation of glucose, the absence of fatty acids from the media and pharmacologic inhibition of fatty acid oxidation in hepatoma cells (Fig. 5B), and 3) pharmacologic inhibition of glucose oxidation lowered  $H_2O_2$  per ATP in bovine aortic endothelial cells (Fig. 5C).

Aerobic metabolism of nutrients for ATP is associated with oxygen radical production and secondary chemical modifications of DNA, lipids, and proteins, potentially accelerating aging (52). Oxygen radicals modify the side chains of lysine, arginine, proline, and histidine residues, resulting in the appearance of protein carbonyl groups, a chemical modification that increases with aging (53). In the present study, reduced protein carbonyl content in Snell dwarf mouse liver is consistent with a decrease in oxygen radical production (Fig. 5A). Other studies also indicate that oxidative damage is reduced in Snell dwarfs. (54, 55).

Our data in hepatoma cells suggest that high glucose utilization can increase oxygen radical levels *in vitro* (Fig. 5B). We raised glucose utilization by increasing the concentration of glucose and reducing the concentration of fatty acids in the media or adding etomoxir, an inhibitor of fatty acid oxidation and stimulator of glucose utilization (56). Etomoxir effects in HepG2 cells support that the reduction of fatty acid utilization elevates oxygen radical damage (57).

Superoxide anions are produced during ATP production by oxidative phosphorylation as electrons from NADH and  $FADH_2$  leak across the inner mitochondrial membrane and react directly with  $O_2$ , forming superoxide, instead of with  $O_2$  and hydrogen ions to form water (58). Hydrogen peroxide ( $H_2O_2$ ) is formed from superoxide anions by superoxide dismutase (59). In bovine aortic endothelial cells, 4-OHCA, an inhibitor of glucose oxidation, lowered  $H_2O_2$  per ATP (Fig. 5C). Energy from glucose metabolism may generate more superoxide anions than fatty acid metabolism, because 1) NADH is oxidized by complex I, the site of highest electron leakage and superoxide anion synthesis and 2) glucose is oxidized by a higher NADH to  $FADH_2$  ratio (60–62). Glucose yields 38 ATP from an NADH to  $FADH_2$  ratio of 10:2 {4 ATP from substrate level phosphorylation (2 by glycolysis, 2 by Krebs cycle), 30 ATP from 10 NADH (2 by glycolysis and 8 by Krebs cycle), and 4 ATP from 2  $FADH_2$  (2 by Krebs cycle)}. Palmitic acid, a long-chain fatty acid, yields 112 ATP from an NADH to

$FADH_2$  ratio of 28:14 {84 ATP from 28 NADH (7 by  $\beta$ -oxidation, 21 by Krebs cycle) and 28 ATP from 14  $FADH_2$  (7 by  $\beta$ -oxidation, 7 by Krebs cycle)}. Fatty acids also activate uncoupling proteins, which reduce oxygen radical production by depolarizing the inner mitochondrial membrane (63). A shift in substrate utilization may underlie the reduction of oxygen radical production in human myotubes exposed to adiponectin (64). However, further research is needed to resolve whether ATP production from glucose is actually a greater source of oxygen radicals than ATP production from fatty acids.

The suppression of glucose utilization in Snell dwarf mice was also linked to the reduction of circulating glucose. In clinical studies, both fasting glucose and hemoglobin A<sub>1c</sub> increase with aging even in the absence of diabetes (65). Thus, we postulated that the reduction of circulating glucose in the long-lived mice may reduce the frequency of glycation. A previous study showed that both circulating glucose and hemoglobin A<sub>1c</sub> are reduced in young calorie restricted rats (66). However, in the present study hemoglobin A<sub>1c</sub> was 4–5% in both Snell dwarf and control mice. We did not check the levels of *N*-carboxymethyllysine, pentosidine, or methylglyoxal to confirm that other glycation end-products were not reduced in Snell dwarfs.

Our measurements of fasting glucose utilization represent the first data obtained by a single injection of [<sup>3</sup>H]glucose in mice. This method shows that fasting glucose utilization in mice is ~10 mg/kg/min. Fasting glucose utilization values obtained by constant infusion of [<sup>3</sup>H]glucose, a widely used technique, tend to be higher. Fasting glucose utilization values may be higher when measured by constant infusion of tracer because of the surgery needed to insert an intravenous catheter into a mouse. After all, elevated carbohydrate metabolism and insulin resistance are characteristic features of the surgical recovery phase (67). The administration of anticoagulants, needed to maintain an open catheter in mice, may also increase carbohydrate metabolism, because anticoagulants, like heparin, disrupt cell-associated lipoprotein lipase activity and can thereby lower fatty acid metabolism (68). These factors may not be an issue when intravenous catheters are used in larger organisms.

Many studies suggest that energy expenditure per unit body weight does not differ between long-lived and control mice. For example, based on daily food intake, the average energy expenditure in Ames dwarf mice and control mice is ~325 cal/kg/min (69). Our measurements indicate that fasting glucose utilization in mice is ~10 mg/kg/min (40 cal/kg/min). Thus, we estimate that fasting glucose utilization accounts for 15–20% of the total daily energy expenditure in control mice and 5–7% in Snell dwarfs. The concept that total energy expenditure per body weight is not reduced in long-lived models is corroborated in calorie restricted rats (70).

In summary, Snell dwarf mice exhibit reduced glucose utilization and elevated fatty acid utilization during fasting. High levels of circulating adiponectin may contribute to the switch in substrate utilization. The reduction of glucose utilization and elevation of fatty acid utilization during fasting may increase

longevity in Snell dwarf mice by decreasing oxygen radical production.

*Acknowledgments*—We thank Dr. P. E. Scherer (University of Texas Southwestern Medical Center) for recombinant adiponectin and rabbit antisera against mouse adiponectin and Dr. B. R. Landau (Case Western Reserve University) for guidance with the isotope enrichment of glucose analysis.

### REFERENCES

- Paolisso, G., Gambardella, A., Ammendola, S., D'Amore, A., Balbi, V., Varricchio, M., and D'Onofrio, F. (1996) *Am. J. Physiol.* **270**, E890–E894
- Al-Regaiey, K. A., Masternak, M. M., Bonkowski, M. S., Panici, J. A., Kopchick, J. J., and Bartke, A. (2007) *J. Gerontol. A. Biol. Sci. Med. Sci.* **62**, 18–26
- Bluher, M., Kahn, B. B., and Kahn, C. R. (2003) *Science* **299**, 572–574
- Holzenberger, M., Dupont, J., Ducos, B., Leneuve, P., Geloën, A., Even, P. C., Cervera, P., and Le Bouc, Y. (2003) *Nature* **421**, 182–187
- Miller, R. A., Buehner, G., Chang, Y., Harper, J. M., Sigler, R., and Smith-Wheelock, M. (2005) *Aging Cell* **4**, 119–125
- Kurosu, H., Yamamoto, M., Clark, J. D., Pastor, J. V., Nandi, A., Gurnani, P., McGuinness, O. P., Chikuda, H., Yamaguchi, M., Kawaguchi, H., Shimomura, I., Takayama, Y., Herz, J., Kahn, C. R., Rosenblatt, K. P., and Kuro-o, M. (2005) *Science* **309**, 1829–1833
- Mirand, E. A., and Osborn, C. M. (1953) *Proc. Soc. Exp. Biol. Med.* **82**, 746–748
- Borg, K. E., Brown-Borg, H. M., and Bartke, A. (1995) *Proc. Soc. Exp. Biol. Med.* **210**, 126–133
- Masoro, E. J., McCarter, R. J., Katz, M. S., and McMahan, C. A. (1992) *J. Gerontol.* **47**, B202–B208
- Barzilai, N., Banerjee, S., Hawkins, M., Chen, W., and Rossetti, L. (1998) *J. Clin. Invest.* **101**, 1353–1361
- Bartke, A., Wright, J. C., Mattison, J. A., Ingram, D. K., Miller, R. A., and Roth, G. S. (2001) *Nature* **414**, 412
- Hauck, S. J., Hunter, W. S., Danilovich, N., Kopchick, J. J., and Bartke, A. (2001) *Exp. Biol. Med. (Maywood)* **226**, 552–558
- Harris, S. B., Gunion, M. W., Rosenthal, M. J., and Walford, R. L. (1994) *Mech. Ageing Dev.* **73**, 209–221
- Berg, A. H., Combs, T. P., Du, X., Brownlee, M., and Scherer, P. E. (2001) *Nat. Med.* **7**, 947–953
- Combs, T. P., Berg, A. H., Obici, S., Scherer, P. E., and Rossetti, L. (2001) *J. Clin. Invest.* **108**, 1875–1881
- Combs, T. P., Pajvani, U. B., Berg, A. H., Lin, Y., Jelicks, L. A., Laplante, M., Nawrocki, A. R., Rajala, M. W., Parlow, A. F., Cheeseboro, L., Ding, Y. Y., Russell, R. G., Lindemann, D., Hartley, A., Baker, G. R., Obici, S., Deshaies, Y., Ludgate, M., Rossetti, L., and Scherer, P. E. (2004) *Endocrinology* **145**, 367–383
- Combs, T. P., Berg, A. H., Rajala, M. W., Klebanov, S., Iyengar, P., Jimenez-Chillaron, J. C., Patti, M. E., Klein, S. L., Weinstein, R. S., and Scherer, P. E. (2003) *Diabetes* **52**, 268–276
- Berryman, D. E., List, E. O., Coschigano, K. T., Behar, K., Kim, J. K., and Kopchick, J. J. (2004) *Growth Horm. IGF Res.* **14**, 309–318
- Tomas, E., Tsao, T. S., Saha, A. K., Murrey, H. E., Zhang, C. C., Itani, S. I., Lodish, H. F., and Ruderman, N. B. (2002) *Proc. Natl. Acad. Sci. U. S. A.* **99**, 16309–16313
- Yamauchi, T., Kamon, J., Minokoshi, Y., Ito, Y., Waki, H., Uchida, S., Yamashita, S., Noda, M., Kita, S., Ueki, K., Eto, K., Akanuma, Y., Froguel, P., Foufelle, F., Ferre, P., Carling, D., Kimura, S., Nagai, R., Kahn, B. B., and Kadowaki, T. (2002) *Nat. Med.* **8**, 1288–1295
- Nawrocki, A. R., Rajala, M. W., Tomas, E., Pajvani, U. B., Saha, A. K., Trumbauer, M. E., Pang, Z., Chen, A. S., Ruderman, N. B., Chen, H., Rossetti, L., and Scherer, P. E. (2006) *J. Biol. Chem.* **281**, 2654–2660
- Beckman, K. B., and Ames, B. N. (1998) *Physiol. Rev.* **78**, 547–581
- Barja, G. (2004) *Trends Neurosci.* **27**, 595–600
- Nishikawa, T., Edelstein, D., Du, X. L., Yamagishi, S., Matsumura, T., Kaneda, Y., Yorek, M. A., Beebe, D., Oates, P. J., Hammes, H. P., Giardino, I., and Brownlee, M. (2000) *Nature* **404**, 787–790
- Fisher, S. J., and Kahn, C. R. (2003) *J. Clin. Invest.* **111**, 463–468
- Cherrington, A. D., Williams, P. E., and Harris, M. S. (1978) *Metabolism* **27**, 787–791
- Baron, A. D., Kolterman, O. G., Bell, J., Mandarino, L. J., and Olefsky, J. M. (1985) *J. Clin. Invest.* **76**, 1782–1788
- Gupta, G., Cases, J. A., She, L., Ma, X. H., Yang, X. M., Hu, M., Wu, J., Rossetti, L., and Barzilai, N. (2000) *Am. J. Physiol.* **278**, E985–E991
- Flurkey, K., Papaconstantinou, J., Miller, R. A., and Harrison, D. E. (2001) *Proc. Natl. Acad. Sci. U. S. A.* **98**, 6736–6741
- Royle, G. T., Wolfe, R. R., and Burke, J. F. (1983) *J. Surg. Res.* **34**, 187–193
- Pinkerton, W. M. (1964) *Proc. Soc. Exp. Biol. Med.* **116**, 959–961
- Shipley, R. A., and Clark, R. E. (1972) *Tracer Methods for In Vivo Kinetics*, Academic Press, New York, pp. 1–20
- Landau, B. R., Wahren, J., Chandramouli, V., Schumann, W. C., Ekberg, K., and Kalhan, S. C. (1996) *J. Clin. Invest.* **98**, 378–385
- Previs, S. F., Hazey, J. W., Diraison, F., Beylot, M., David, F., and Brunen-graber, H. (1996) *J. Mass Spectrom.* **31**, 639–642
- Lang, C. H., Bagby, G. J., Buday, A. Z., and Spitzer, J. J. (1987) *Metabolism* **36**, 180–187
- Woods, A., Azzout-Marniche, D., Foretz, M., Stein, S. C., Lemarchand, P., Ferre, P., Foufelle, F., and Carling, D. (2000) *Mol. Cell. Biol.* **20**, 6704–6711
- da Costa, K. A., Cochary, E. F., Blusztajn, J. K., Garner, S. C., and Zeisel, S. H. (1993) *J. Biol. Chem.* **268**, 2100–2105
- Levine, R. L., Garland, D., Oliver, C. N., Amici, A., Climent, I., Lenz, A. G., Ahn, B. W., Shaltiel, S., and Stadtman, E. R. (1990) *Methods Enzymol.* **186**, 464–478
- Li, L. O., Mashek, D. G., An, J., Doughman, S. D., Newgard, C. B., and Coleman, R. A. (2006) *J. Biol. Chem.* **281**, 37246–37255
- DeFronzo, R. A., Jacot, E., Jequier, E., Maeder, E., Wahren, J., and Felber, J. P. (1981) *Diabetes* **30**, 1000–1007
- Rossetti, L., Stenbit, A. E., Chen, W., Hu, M., Barzilai, N., Katz, E. B., and Charron, M. J. (1997) *J. Clin. Invest.* **100**, 1831–1839
- Itoh, Y., Esaki, T., Kaneshige, M., Suzuki, H., Cook, M., Sokoloff, L., Cheng, S. Y., and Nunez, J. (2001) *Proc. Natl. Acad. Sci. U. S. A.* **98**, 9913–9918
- Rossetti, L., Frontoni, S., Dimarchi, R., DeFronzo, R. A., and Giaccari, A. (1991) *Diabetes* **40**, 444–448
- Verdonk, C. A., Rizza, R. A., and Gerich, J. E. (1981) *Diabetes* **30**, 535–537
- Basu, R., Schwenk, W. F., and Rizza, R. A. (2004) *Am. J. Physiol.* **287**, E55–E62
- Gastaldelli, A., Miyazaki, Y., Pettiti, M., Buzzigoli, E., Mahankali, S., Ferrannini, E., and DeFronzo, R. A. (2004) *J. Clin. Endocrinol. Metab.* **89**, 3914–3921
- Natali, A., and Ferrannini, E. (2006) *Diabetologia* **49**, 434–441
- Combs, T. P., Wagner, J. A., Berger, J., Doebber, T., Wang, W. J., Zhang, B. B., Tanen, M., Berg, A. H., O'Rahilly, S., Savage, D. B., Chatterjee, K., Weiss, S., Larson, P. J., Gottesdiener, K. M., Gertz, B. J., Charron, M. J., Scherer, P. E., and Moller, D. E. (2002) *Endocrinology* **143**, 998–1007
- Andreelli, F., Foretz, M., Knauf, C., Cani, P. D., Perrin, C., Iglesias, M. A., Pillot, B., Bado, A., Tronche, F., Mithieux, G., Vaulont, S., Burcelin, R., and Viollet, B. (2006) *Endocrinology* **147**, 2432–2441
- Witters, L. A., Nordlund, A. C., and Marshall, L. (1991) *Biochem. Biophys. Res. Commun.* **181**, 1486–1492
- Stauber, A. J., Brown-Borg, H., Liu, J., Waalkes, M. P., Laughter, A., Staben, R. A., Coley, J. C., Swanson, C., Voss, K. A., Kopchick, J. J., and Corton, J. C. (2005) *Mol. Pharmacol.* **67**, 681–694
- Balaban, R. S., Nemoto, S., and Finkel, T. (2005) *Cell* **120**, 483–495
- Stadtman, E. R. (2006) *Free Radic. Res.* **40**, 1250–1258
- Hsieh, C. C., and Papaconstantinou, J. (2006) *FASEB J.* **20**, 259–268
- Leiser, S. F., Salmon, A. B., and Miller, R. A. (2006) *Mech. Ageing Dev.* **127**, 821–829
- Kruszynska, Y. T., and Sherratt, H. S. (1987) *Biochem. Pharmacol.* **36**, 3917–3921
- Merrill, C. L., Ni, H., Yoon, L. W., Tirmenstein, M. A., Narayanan, P., Benavides, G. R., Easton, M. J., Creech, D. R., Hu, C. X., McFarland, D. C., Hahn, L. M., Thomas, H. C., and Morgan, K. T. (2002) *Toxicol. Sci.* **68**, 93–101
- Turrens, J. F. (2003) *J. Physiol.* **552**, 335–344



59. Liochev, S. I., and Fridovich, I. (2007) *Free Radic. Biol. Med.* **42**, 1465–1469
60. Barja, G., and Herrero, A. (1998) *J. Bioenerg. Biomembr.* **30**, 235–243
61. Kushnareva, Y., Murphy, A. N., and Andreyev, A. (2002) *Biochem. J.* **368**, 545–553
62. Grivennikova, V. G., and Vinogradov, A. D. (2006) *Biochim. Biophys. Acta* **1757**, 553–561
63. Boss, O., Muzzin, P., and Giacobino, J. P. (1998) *Eur. J. Endocrinol.* **139**, 1–9
64. Civitarese, A. E., Ukropcova, B., Carling, S., Hulver, M., DeFronzo, R. A., Mandarino, L., Ravussin, E., and Smith, S. R. (2006) *Cell Metab.* **4**, 75–87
65. Elahi, D., and Muller, D. C. (2000) *Eur. J. Clin. Nutr.* **54**, Suppl. 3, S112–S120
66. Masoro, E. J., Katz, M. S., and McMahan, C. A. (1989) *J. Gerontol.* **44**, B20–B22
67. Hill, A. G., and Hill, G. L. (1998) *Br. J. Surg.* **85**, 884–890
68. Knutson, V. P. (2000) *Endocrinology* **141**, 693–701
69. Mattison, J. A., Wright, C., Bronson, R. T., Roth, G. S., Ingram, D. K., and Bartke, A. (2000) *J. Am. Aging Assoc.* **23**, 9–16
70. McCarter, R., Masoro, E. J., and Yu, B. P. (1985) *Am. J. Physiol.* **248**, E488–E490